

Plasma Spray: Study of the Coating Generation

P. Fauchais, M. Vardelle, A. Vardelle & L. Bianchi*

University of Limoges, Laboratoire Céramiques Nouvelles et Traitements de Surface, URA 320-CNRS-Equipe Plasma, Laser, Matériaux, 123 Avenue Albert Thomas, 87060, Limoges Cedex, France

*CEA-DAM BIII, B.P. 12, 91680 Bruyeres-le-Châtel, France

(Received 6 June 1995; accepted 25 July 1995)

Abstract: A plasma sprayed coating is built up particle by particle, resulting in a coating with a layered structure that is highly anisotropic. The spray parameters affect certain factors of the coating, such as the size and distribution of porosity, oxide content, residual stresses, macro and microcracks, factors which have an important influence on the performance and eventual failure of the coating. Many works (modelling and measurements) have been devoted to the particles in flight and how these parameters are influenced by the plasma jets and particle injection macroscopic parameters.

However, there is a shortage of published information on the way the particles spread upon impact and solidify on the substrate or the previously deposited layers and how these phenomena are connected to the deposit microstructure. This paper was concerned with expanding our knowledge in this field by concentrating on the following:

- modelling of deformation and solidification of a droplet on a substrate;
- measurement of the splat formation and cooling;
- experimental results and comparison with models.

1 INTRODUCTION

Thermal spraying allows one to solve many problems of wear, corrosion, thermal cycling, etc., by using a thin layer of a specific material (coating) sprayed on the component surface without degrading the mechanical properties of the substrate. Plasma spraying has extended drastically the capabilities of the thermal spray coatings by accommodating materials with very high melting points, such as ceramics, cermets, refractory alloys and superalloys, and it is now a permanent part of the mechanical engineering discipline.^{1–4}

For a long time scientific research has lagged behind the technical applications due to the complexity of the involved phenomena. The coating, generated splat by splat with particles impacting on already solidified ones, exhibits a layered structure

that is highly anisotropic.⁵ The velocity and molten state of the particles upon impact depend on their trajectories in the plasma jet. However, as the particles have size and injection velocity distributions they have widely different trajectories and thus momentum and temperature histories, their heat treatment being complicated by heat propagation and evaporation phenomena.⁶ Such particle velocity and temperature distributions upon impact affect the coating thermomechanical properties through the size and distribution of porosity, oxide content, residual stresses, macro and microcracks, real contacts between the piled splats.^{5,7} Thus a basic understanding of plasma sprayed coating formation requires the knowledge of the thermal history of the droplets during their flattening and cooling process. Although many studies have recently been devoted to the plasma jets and particles in flight (see the recent reviews^{8–10}), the splat formation has received much less attention¹¹ and this paper will try to expand our knowledge in this

*L. Bianchi will leave CEA in July then correspondence should be sent to Limoges

field. First the theories of deformation and solidification of a droplet impacting on a substrate, as well as the coating generation models, will be presented, then the different experimental techniques to characterize qualitatively and quantitatively the splat formation will be described, and finally the recent results obtained for alumina or zirconia particles flattening and cooling, as well as the correlations with the corresponding coating properties, will be discussed.

2 MODELLING OF DEFORMATION AND SOLIDIFICATION OF A DROPLET ON A SUBSTRATE

2.1 Flattening degree

Many studies have been devoted to this problem, which is also that of splat-quench solidification. Recently, Bennett and Poulikakos¹² have reviewed the different models allowing one to calculate the degree of flattening of such droplets. All the models deal with flat substrates and start with an energy balance stating that the initial kinetic energy of the impacting droplet is dissipated as viscous energy and surface tension energy. They are all expressed in terms of particle Reynold's number ($Re = \rho u d / \mu$, where ρ , μ , u and d are, respectively, the liquid density and viscosity, and the particle velocity and diameter) and Weber's number ($We = \rho u^2 d / \sigma$, where σ is the liquid vapour surface tension). For spraying, one of the most popular models is that of Madejski¹³ relating the ratio $D/d = \xi$ (where D is the splat diameter, assumed to be a disk, and d the spherical droplet diameter) to Re and We by:

$$\frac{3\xi^2}{We} + \frac{1}{Re} \left(\frac{\xi}{1.2941} \right)^5 = 1 \quad (1)$$

However, as for alumina or zirconia plasma sprayed particles, the We values are extremely high (10^2 – $2 \cdot 10^4$), at least when the flattening starts, ξ being lower than 6, eqn (1) reduces to the well known expression:

$$\xi = 1.2941 Re^{0.2} \quad (2)$$

It is worth noting that eqn (2) does not account for the wettability of the substrate for which Bennett and Poulikakos¹² have suggested the following modification to eqn (1):

$$\frac{1}{Re} \left(\frac{\xi}{1.2941} \right)^5 + 3 \frac{[(1 - \cos \Theta_e) \xi^2 - 4]}{We} = 1 \quad (3)$$

where Θ_e is the equilibrium contact angle between the liquid and the substrate. However, if this model modifies deeply the flattening behaviour for $We < 200$, it does not change anything in the viscous dissipation domain ($We > 1000$). The sophisticated model of Watanabe *et al.*,¹⁴ neglecting the surface tension and writing continuity, momentum and energy equations, shows that:

$$\xi = 0.82 Re^{0.2} \quad (4)$$

It allows one to calculate a normalized flattening time τ_d :

$$\tau_d = 0.31 Re^{0.2} \quad (5)$$

Similar calculations were introduced by Trapaga and Szekely,¹⁵ Lin *et al.*^{16,17} and Bertagnolli *et al.*,¹⁸ all these authors neglected the particle substrate wettability to calculate the particle flattening. However, such models explain why at the end of the spreading in certain conditions the liquid flows almost parallel to the substrate, limiting the effective contact area between the splat and the substrate. Thus, upon cooling the peripheral part of the splat detaches from the substrate surface as confirmed by crystallographic characterization of a single splat.^{19,20} Such findings also raise questions about the validity of the method because probably, at the end of flattening when the liquid flows parallel to the substrate, the surface tension and wettability play a role that should be taken into account in the models as shown by the experimental results.

A different approach was introduced by Houben²¹ and by Shnakov and Ermakov,²² who accounted for shock waves generated in the flattening particle. It allowed Houben to explain, at least qualitatively, the different shapes of plasma sprayed molybdenum splats, but here again wettability was not introduced.

2.2 Cooling down of the splats

The variables with the greatest influence on the splat-cooling rate are splat thickness e , interface heat transfer coefficient h or thermal contact resistance R and instantaneous splat temperature.²³ The use of classical theories of nucleation and growth, solving simultaneously the heat flow and solidification problems, allow one to predict the morphological characteristics of the splat structures.²⁴ According to eqns (2) or (4) it is clear that the final thickness of the splats will be directly linked to the particle Re , i.e. to the velocity, diameter and particle viscosity upon impact ($\mu \sim$

$\exp\left(\frac{E}{pT}\right)$ implies a fast increase of Re with T as soon as $T > T_m$ (melting temperature). The first models have assumed that splat cooling started when flattening was terminated but it is not necessarily the case, especially when the splat is very thin.¹⁸ However, Bertagnoli *et al.*¹⁸ have shown that, even when the flattening and freezing cannot be treated as separate processes, the influence of the solidification on the spreading is, in most cases, not significant. The high velocities of the flowing material develop in the upper part of the cooling lamella, thus the spreading time and the related splat size are nearly the same when considering or not the interaction of heat and fluid flow during flattening. It is important to underline that with the choice of h or R , for example assumed to vary between 10^{-8} and 10^{-4} $K.m^2.W^{-1}$, the models introduce a new unknown related to the contact between the splat and the substrate or the previously deposited layers, contact which depends on wettability. For zirconia splats the importance of the splat thickness on the cooling time of the splats is illustrated²⁵ in Fig. 1(a) for different values of R and in Fig. 1(b) for two substrate materials (zirconia and steel). In both figures the importance of the splat thickness is obvious. When R increases from 10^{-7} to 10^{-6} $K.m^2.W^{-1}$, cooling is slowed down drastically, while there is almost no difference between the values obtained with $R = 10^{-7}$ or 10^{-8} . As shown in Fig. 1(b) the effusivity of the substrate also plays an important role, the cooling down being much slower with a zirconia substrate than with a steel one.

2.3 Modelling of the coating generation

Once the description of the particle on arrival at the substrate or previously deposited layers has been considered it is possible to define a set of physically-based rules for combining these events to obtain a coating. For example, Knotek and Elsing²⁶ have constructed a model assuming that pores have been created between the splats without any other generation mechanism. Fukunuma²⁷

tried to include trapping of the plasma gas. Cirolini *et al.*,²⁸ and then Harding *et al.*,²⁹ described the growth of the coating by a stochastic process, the surface roughness by a fractal and they took into account the surface temperature evolution. However, the basis of these models is the splat shape and dimensions (see Section 2.1) and, for example, the use of eqn (4) instead of eqn (2) can modify the obtained porosity by a factor of 2.²⁹

3 MEASUREMENT OF THE SPLAT FORMATION AND COOLING

Various studies have been devoted to the way particles flatten on flat, cold substrates and they are summarized in Ref. 11.

3.1 Qualitative measurements

Russian workers^{30–32} have made a detailed description of alumina splats. For a given spraying condition, due to the widely different trajectories of the particles, they have registered more than 30 different splat shapes from almost unmolten particles stuck to the surface to completely exploded overheated particles. If some of the splats exhibited the disk shape used in modelling it was more an exception than a rule and many were “star-like” particles with strong disruption and fragmentation of material at the splat periphery, sometimes with discontinuity in the centre, or “sombbrero” particles with an unmolten core at the splat centre.

When sprayed on rough surfaces the spreading of the droplets is limited by the irregularities of the surface, resulting in smaller and thicker splats than on flat substrates — however, their observation, even with SEM, is not very easy.

3.2 Semi-quantitative measurements

A test procedure was developed by Roberts and Clyne³³ to collect the splats on a substrate

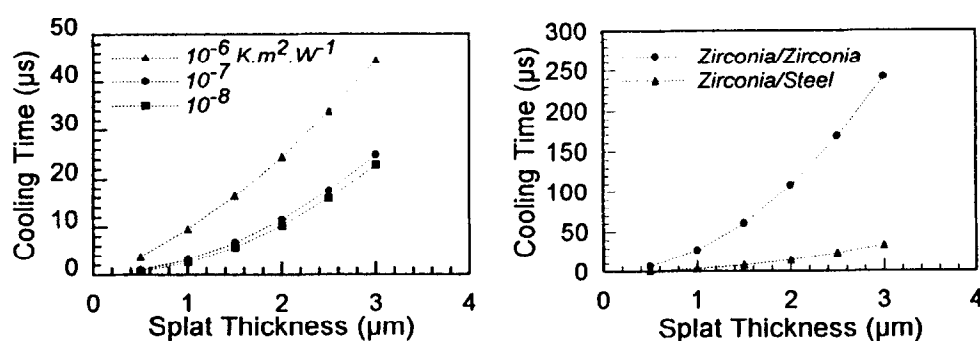


Fig. 1. Evolution of the cooling rate of zirconia splats versus splat thickness for different thermal contact resistances (a) and substrate natures (b).

traversed behind a screen containing a slit, while the spray gun was traversed in the opposite direction in front. It has allowed the determination of the mean splat diameter and inter-splat spacing as a function of position within the spray cone. This test has been improved at the laboratory^{34,35} by using flat plates of different materials, heated at different temperatures by a radiative heating system, the plasma jet flux being almost suppressed by the water-cooled screen and the narrow slit (1 mm width). The image analysis of the splats (about 5000), collected at different points of the spray cone, allowed us to determine their diameter d and shape factor SF distributions ($SF = p^2/(4\pi \cdot S)$, where p is the splat perimeter and S its area, with $SF = 1$ corresponding to a perfect disk. However, with this systematic analysis, part of the splat, when its shape is too much distorted, can be eliminated.

3.3 Quantitative measurements

A fast (100 ns) pyrometer,³⁶ developed at the laboratory and at the industrial Materials Institute of NRC at Boucherville Canada, and focused on a small spot on the substrate surface has allowed us to monitor the flattening of the particles and then the splat cooling down. It has been modified^{37,38} to determine also the velocity, surface temperature and diameter of a single particle prior to its impact. It consisted of two double wavelengths optical fibre pyrometers, one being focused 2 mm before the substrate and the other on a small spot on the substrate. It allowed us to determine the flattening time and flattening degree of the particle, as well as the cooling rate of the splat.

However, it is worth noting that many parameters can affect the precision of the measurements:

- finite time-response of the detection system³⁹ (in our case 5 ns);
- deviation from grey body behaviour of the radiating surface;
- detection of plasma light reflected on the substrate or particle surface;
- presence of temperature gradients at the particle surface;
- cooling rates higher than 250 K/ μ s resulting in a maximum signal intensity reached before the end of the flattening process, leading to a decrease in the apparent flattening time.⁴⁰

It is also important to underline that, when considering the surface variation of the flattening particle, such a device allows one to determine it whatever its shape may be, provided that all the

material of the splat remains in the field of view of the pyrometer.

4 EXPERIMENTAL RESULTS AND COMPARISON WITH MODELS

4.1 Experimental conditions

The results presented in the following were obtained with alumina and zirconia particles ($-45 + 22 \mu\text{m}$ fused and crushed). The substrates were made of stainless steel 304 L, polished: $Ra \sim 0.1 \mu\text{m}$ or sand blasted: $Ra \sim 3 \mu\text{m}$; or of plasma sprayed alumina or zirconia coatings, polished: $Ra \sim 0.4 \mu\text{m}$. They were sprayed either with a 7 or 10 mm i.d. nozzle dc plasma torch or an RF plasma torch (Tekna PL50) with internal diameter of 50 mm.^{35,41} The dc torches worked with 40 kW, 15 slm H_2 and 45 slm Ar and the RF torch with 47 kW, 50 slm Ar in the central gas and 90 slm Ar and 10 slm H_2 in the sheath gas. With such conditions for alumina particles, the velocities of the particles were ranging between 300 m/s and 50 m/s.^{42,35}

Coatings were sprayed on disk shaped samples ($d = 25 \text{ mm}$, $e = 4 \text{ mm}$) disposed on a rotating substrate holder ($d = 110 \text{ mm}$) with the torches moved parallel to the cylinder axis. In all cases the bead overlapping was 1/2 and the substrates were either preheated or not during spraying, their temperature, measured with an IR pyrometer, being controlled by air jets.

4.2 Splat shapes

4.2.1 Influence of the substrate temperature

In the following will be presented only the diameter and shape factor distributions of alumina particles sprayed on smooth stainless steel, the results being quite similar for zirconia particles. Figures 2 and 3 are related to splats obtained with the 7 mm, i.d. dc torch. Figure 2 is relative to a cold substrate (75°C) and Fig. 3 to a hot one (300°C).

The mean diameter d of particles is bigger with the hot substrate (compare Fig. 2(a) and Fig. 3(a)), but the most spectacular effect of the substrate temperature is on the shape factor SF (compare Fig. 2(b) and Fig. 3(b)). For the cold substrate, $SF \sim 0.6$ (very distorted shapes) and rather different shapes are obtained depending on the splat position in the spray cone, while for the hot substrate, $SF \sim 0.92$ and this shape is observed whatever the splat position may be within the spray cone. This corresponds to splats having a perfect lenticular shape as shown in Fig. 4 and a very regular cross

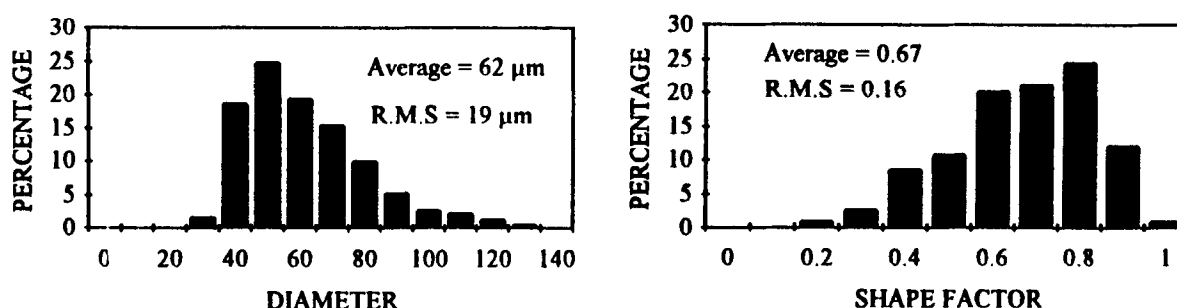


Fig. 2. Splat characteristics determined from all the splats collected in the sprayed spot on a smooth ($R_a \sim 0.4 \mu\text{m}$) steel (304L) substrate at a temperature $T_s = 75^\circ\text{C}$. (a) Diameter distribution. (b) Shape factor distribution.

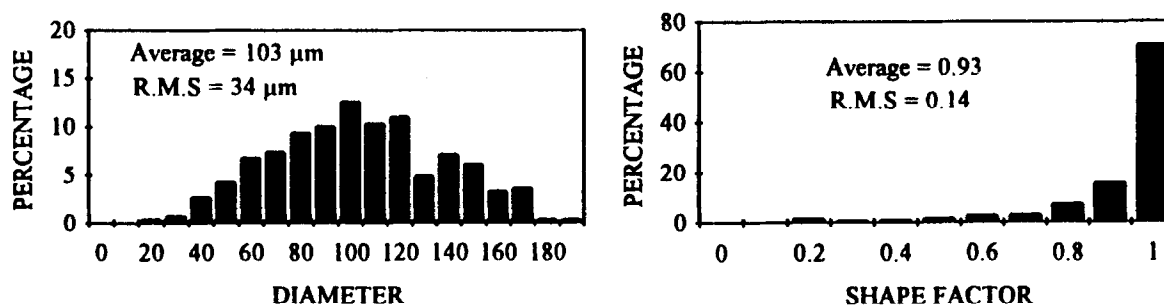


Fig. 3. Splat characteristics determined from all the splats collected in the sprayed spot on a smooth ($R_a \sim 0.4 \mu\text{m}$) steel (304L) substrate at a temperature $T_s = 300^\circ\text{C}$. (a) Diameter distribution. (b) Shape factor distribution.

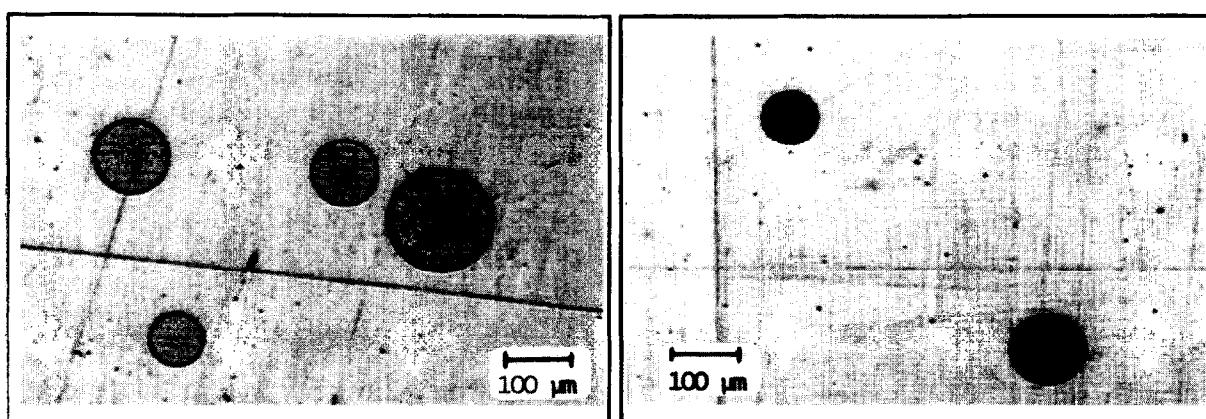


Fig. 4. Zirconia splats obtained on a smooth ($R_a \sim 0.2 \mu\text{m}$) steel substrate at 300°C with (a) a dc torch (7 mm i.d. nozzle) and (b) an RF plasma torch.

section with a “bat-man” profile showing a little thicker rim. The excellent mechanical contact between the splat and the substrate is illustrated by the microcracks network covering its whole surface and due to the quenching stresses relaxation. When spraying on a cold substrate at high velocity the particle is not too far from a lenticular shape but with many fingers extending far away from it (see Fig. 5(a)). With a low impact velocity (RF spraying) the splat is extensively fingered (see Fig. 5(b)), which is due to the flow, after flattening, of the molten material of a rather thick splat which is cooled down much less rapidly than the splat obtained at high velocity. This explains the reduction of d with the cold substrate due to the “splashing” of the particles.

When spraying either alumina on polished sprayed alumina or zirconia on polished sprayed zirconia a similar phenomenon has been observed with close to disk-shaped splats on hot substrates. As previously underlined,³⁴ as soon as the metallic substrate is oxidized (when heated in air for more than 12 min at 300°C) the SF of the splats is again that obtained at low temperature. The SF does not depend on the particle velocity, an SF close to one being obtained with the three spraying conditions for a hot, flat, non-oxidized substrate (hot means a temperature over 200°C).

4.2.2 Influence of the particle velocity

The measurements have been systematically performed with hot smooth steel substrates because

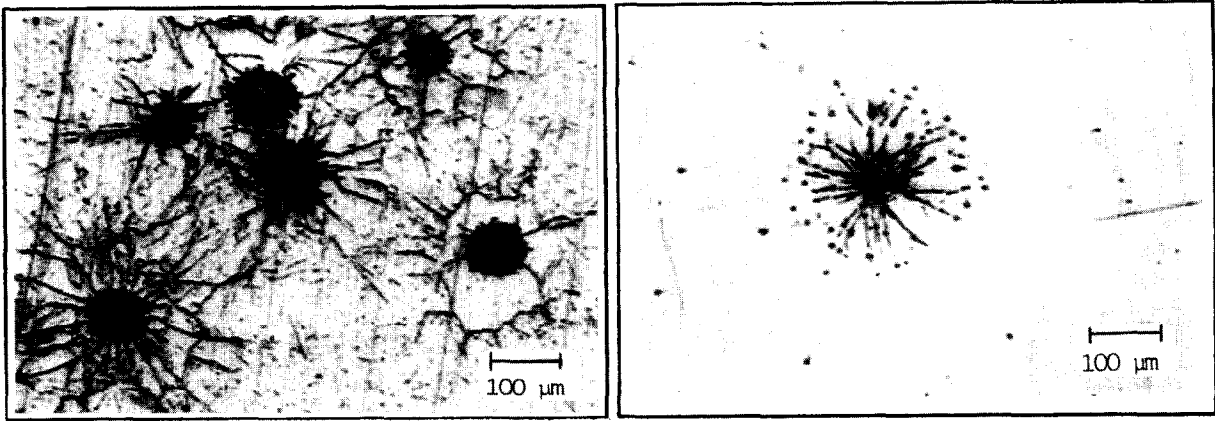


Fig. 5. Zirconia splats obtained on a smooth ($R_a \sim 0.2 \mu\text{m}$) steel substrate at 75°C with (a) a dc torch (7 mm i.d. nozzle) and (b) an RF plasma torch.

the obtained disk-shaped splats allowed us to determine precisely their thickness which was not possible for extensively fingered splats. Table 1 summarizes the results for zirconia splats.

It is interesting to underline that when spraying on cold substrates the lowest values of the SF are obtained with low velocity particles. This is probably due to the highest thickness of the splats which allow the molten material to flow very easily parallel to the substrate surface at the end of the particle flattening. On hot substrates the SF is close to one but, according to the thicker splat resulting in a lower cooling rate, the rounded rim is thicker and larger due to the surface tension effects (see Fig. 4(b)).

4.2.3 Influence of the substrate roughness

Due to the difficulties in observing the splats on a rough surface, even when using back scattered electrons with SEM, only a few images have been examined and no statistical treatment has been performed as in the case of smooth substrates. As already pointed out by Moreau *et al.*,⁴³ the flattening degree of the splats decreases with the substrate roughness. This is due to the asperities of the surface limiting the material flow. However, the substrate temperature effect is still there, as shown in Fig. 6(a) and Fig. 6(b). Figure 6(a) corresponds to a splat collected on a rough 304L steel substrate

($R_a \sim 3 \mu\text{m}$, $R_t \sim 20 \mu\text{m}$) kept at 75°C . The splat exhibits disruption and fragmentation of the material at its periphery with a large material discontinuity at its centre. Contrarily to the splats shown in Fig. 4 no microcracks can be seen, probably due to the poor contact between the splat and the rough surface. The splat shape obtained on the hot substrate (300°C) is quite different (see Fig. 6(b)). Of course it no longer has the lenticular shape obtained with the smooth substrate but most of the material has been kept in the splat. A few pores, probably due to the escape of the gas entrapped in the asperities under the splat, can be seen. Very few microcracks are observed. This might be due to a weaker contact than in the case of a smooth substrate and also to the ability of the surface peaks and valley to accommodate deformation. The mean surface of the splats collected on hot and rough substrates is smaller than that obtained on smooth substrates — in the same spraying conditions $d = 50 \pm 20 \mu\text{m}$ against $103 \pm 33 \mu\text{m}$. However, even if wettability is not clearly defined on rough surfaces, the results illustrated in Fig. 5 show clearly there is an effect which can be called wettability.

4.3 Evolution of flattening time and degree and cooling rate

4.3.1 Smooth substrates

Measurements were only performed with the two dc plasma torches corresponding, for zirconia particles, to a velocity range of 100–300 m/s and surface temperatures between 2400 and 4500 K, and the results from Ref. 35 are summarized in Table 2.

According to the precision of the measurements the flattening time (mostly controlled by the kinetic energy of the particle) is about the same on cold and hot substrates. The difference in flattening degree is probably due to the fact that on cold substrates part of the material splashes away from

Table 1. Splats flattening degree, mean diameter and thickness for three mean velocities upon impact

Nozzle diameter (mm)	7	10	50
Type of torch	dc	dc	RF
Mean velocity at stand-off distance (m/s)	200	135	35
Shape factors	0.93	0.93	0.98
Splat mean diameter (μm)	103 ± 33	92 ± 31	76 ± 22
Splat mean thickness (μm)	0.85 ± 0.4	1.1 ± 0.5	2.4 ± 0.9
Flattening degree	5.0	4.6	3.6

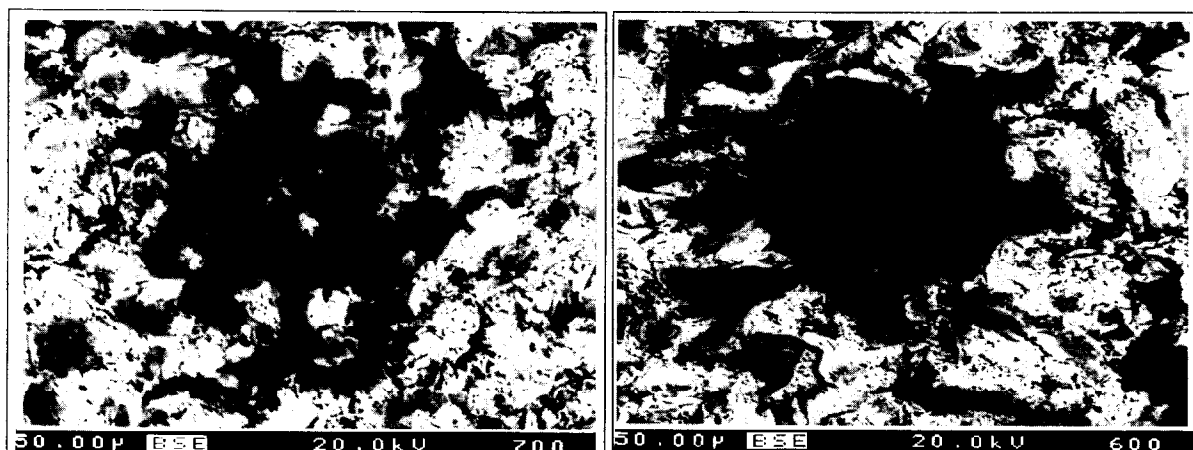


Fig. 6. Alumina splats from a dc plasma torch (7 mm in i.d.) collected on rough surfaces ($R_a \sim 3 \mu\text{m}$) with surface temperature at (a) 75°C and (b) 300°C.

Table 2. Flattening time and degree and cooling rate for zirconia particles ($-45 + 22 \mu\text{m}$) sprayed on hot and cold stainless steel smooth substrates

	Flattening time (μs)	Flattening degree	Cooling rate ($\text{K}/\mu\text{s}$)	Particle velocity (m/s)	Splat thickness
Cold substrate 750°C	0.5–1	2–6	100–200	100–300	—
Hot substrate 300°C	0.5–1	4–6	400–800	100–300	1.5–0.6

the splat and is not necessarily accounted for by the measuring set-up (see Section 3.3). The differences in cooling rates are mainly due to the much better mechanical contact when particles are sprayed on hot substrates (see Fig. 4). Calculated temperature evolution of the splats upon cooling fit well the experimental curves on hot substrates, with $R = 4$ to $6 \times 10^{-7} \text{ K.m}^2.\text{W}^{-1}$ against $R = 3$ to $5 \times 10^{-6} \text{ K.m}^2.\text{W}^{-1}$ on cold substrates.²⁵ Such cooling rates are also in good agreement with the splat thicknesses measured on hot substrates. When calculating the flattening degree versus the Reynolds number (assuming a temperature evolution of the zirconia viscosity similar to that of alumina³⁵), two different results are found:³⁵ for hot substrates $D/d = 1.294 \text{ Re}^{0.2}$, which is almost the correlation of Madejski,¹³ for cold substrates $D/d = 0.83 \text{ Re}^{0.2}$.

Such a result is in good accordance with that found for the mean splat diameter (see Section 4.2.1) and is due to the material splashing on cold substrates reducing the apparent final surface of the splat.

Finally, it is worth noting that when spraying on oxidized hot substrates the cooling rate, with a mean value of $100 \text{ K}/\mu\text{s}$, is even a little bit lower than that obtained with a cold substrate.

4.3.2 Rough substrates

The measurements are still in progress at the laboratory and the only measurements performed

on such substrates are those of Moreau *et al.*⁴³ related to Mo particles on glass substrates, with roughness varying from $0.02 \mu\text{m}$ (smooth) to $9.6 \mu\text{m}$ (coarse). The flattening degree decreased from 7.4 on the smooth surface to 3.9 on the coarse, gritblasted one in good accordance with the previously presented results (see Section 4.2.3). Similarly, the cooling time increased from 3 to $10 \mu\text{s}$.

Even if the influence of all these parameters is far from being completely known, their influence on the coatings properties is obvious, as demonstrated by Bianchi *et al.*⁴¹ The coating adhesion increases drastically with hot substrates (up to three times for zirconia) and high velocity particles, intermediate results being obtained with hot substrates and low velocity particles (RF spraying).

5 CONCLUSIONS

Flattening and solidification of plasma sprayed particles impinging on a substrate surface are very complex phenomena involving rapid changes in the dynamic and thermal state of the molten particles that depend on many factors. All the models, even those taking into account shock waves, deal with smooth substrates and neglect depth wettability. If they predict within 30% the flattening degree and time, they fail to predict the cooling rate of the

splat except through different values of the thermal contact resistance introduced arbitrarily. The new techniques developed to study on the one hand the splat diameters and shape factors distributions on smooth substrates (derived from line scan test) and on the other the flattening degree and time, the splat cooling rate versus the velocity, diameter and surface temperature of a single impacting droplet, have brought new insights on the influence of the substrate characteristics on the splat formation. For alumina and zirconia particles impacting on smooth substrates ($R_a < 0.2 \mu\text{m}$) metallic or ceramic (polished sprayed alumina or zirconia coatings), the substrate temperature has a drastic influence. Below 150–200°C, the splats are extensively fingered corresponding to poor wettability and adhesion, the worst results being obtained for low velocity particles (RF spraying). Over these temperatures (provided the metallic surface is not oxidized) the shape of the splats, whatever their position within the spray cone may be, is almost perfectly lenticular. In this case there is an excellent contact with the substrate as shown by the micro-cracks network covering almost the whole splat surface (especially for particles sprayed at high velocity) and the very fast cooling rate of the splats (between 400 and 800 K/ μs against 100–200 K/ μs for the same splats on cold substrates). Such a good contact is probably due to a much better wettability. A high velocity reduces the splat thickness and increases the cooling rate. On rough substrates the measurements are still in progress, but a similar phenomenon is observed when the substrate is heated over 150–200°C, the size of the splat being smaller, with the surface asperities reducing the material flow and its thickness being correspondingly higher than in the case of smooth substrates. Measurements, performed with molybdenum particles, show that the cooling time is also reduced. Such results are in good agreement with the measurements of cohesion/adhesion of the coatings which values, for the same particle velocities range, increase almost by a factor of three when coatings are sprayed at 250°C (with substrate preheating) and decrease, for the same substrate temperature, when particle velocity decreases.

Such results mean that much work is still necessary to improve the models by taking into account wettability (probably at the end of the spreading) and roughness and to complete the measurements, especially on rough surfaces. They will allow, later on, the construction of more reliable models for coating generation provided the temperature evolutions during the beads and passes formation are taken into account.

REFERENCES

1. American Welding Society (Pub.). *Thermal Spraying*. Am. Welding Soc., Miami, FL, USA, 1985.
2. FAUCHAIS, P., GRIMAUD, A., VARDELLE, A. & VARDELLE, M., *Ann. Phys. Fr.*, **14** (1989) 269.
3. SMITH, R. W. & NOVAK, R., *Powder Metall. Int.*, **23**(3) (1991) 147.
4. FAUCHAIS, P. & VARDELLE, M., *Pure Appl. Chem.*, **64**(9) (1992) 63.
5. McPHERSON, R., *Surf. Coat. Technol.*, **(39/40)** (1989) 173.
6. BOULOS, M., FAUCHAIS, P., PFENDER, E. & VARDELLE, M., Fundamentals of plasma particle momentum and heat transfer. In *Thermal Spraying*, World Scientific, 1993, p.3.
7. McPHERSON, R., *Thin Solid Films*, **83** (1981) 297.
8. FAUCHAIS, P., COUDERT, J. F. & VARDELLE, M., In *Plasma Diagnostics*, Academic Press Inc., 1989, p.349.
9. FAUCHAIS, P., COUDERT, J. F., VARDELLE, A., VARDELLE, M. & DENOIRJEAN, A., *J. Thermal Spray Technol.*, **1**(2) (1992) 117.
10. VARDELLE, M., VARDELLE, A. & FAUCHAIS, P., *J. Thermal Spray Technol.*, **2**(1) (1993) 79.
11. VARDELLE, A., VARDELLE, M. & FAUCHAIS, P., *Pure Appl. Chem.*, **64**(5) (1992) 637.
12. BENNETT, T. & POULIKAKOS, D., *J. Mater. Sci.*, **28** (1993) 963.
13. MADEJSKI, J., *Int. J. Heat Mass Transfer*, **19** (1976) 1009.
14. WATANABE, T., KURIBAGASHI, I., HONDA, T. & KANZAWA, A., *Chem. Eng. Sci.*, **47**(12) (1992) 3059.
15. TRAPAGA, G. & SZEKELY, J., *Metall. Trans.*, **B22** (1991) 901.
16. LIN, H., LAVERNIA, E. J. & RANGEL, R. H., *J. Thermal Spray Technol.*, **2**(4) (1993) 369.
17. LIN, H., LAVERNIA, E. J. & RANGEL, R. H., *J. Phys. D, Appl. Phys.*, **26** (1993) 1900.
18. BERTAGNOLLI, M., MARCHESE, M. & JACUCCI, G., *J. Thermal Spray Technol.*, **4**(1) (1995) 41.
19. SAFAI, S. & HERMAN, H., *Thin Solid Films*, **45** (1977) 295.
20. McPHERSON, R. & SHAFER, V., *Thin Solid Films*, **97** (1982) 201.
21. HOUBEN, J. M., Doctoral thesis, University of Eindhoven, The Netherlands, 1988.
22. SHNAKOV, A. M. & ERMAKOV, S. S., *Fizika i Khimiya Obrabotki Materialov*, **20**(3) (1986) 66.
23. RUHL, R. C., *Mater. Sci. Eng.*, **1** (1967) 313.
24. BOSWELL, P. G., *Metals Forum*, **2**(1) (1979) 40.
25. VARDELLE, A., GOBIN, D., VARDELLE, M., LÉGER, A. C. & FAUCHAIS, P., *J. Thermal Spray Technol.*, **4**(1) (1995) 50.
26. KNOTEK, O. & ELSING, R., *Surface Coat. Technol.*, **32** (1987) 261.
27. FUKANUMA, H., In *ASM Int. ASM*, OH, USA, 1992, p.767.
28. CIROLINI, S., HARDING, J. H. & JACUCCI, G., *Surface Coat. Technol.*, **48** (1991) 137.
29. HARDING, J. H., MULHERAN, P., CIROLINI, S., MARCHESE, M. & JACUCCI, G., *J. Thermal Spray Technol.*, **4**(1) (1995) 54.
30. SOLOLENKO, O. P. & FEDORCHENKO, A. I., In *High Temperature Dust Laden Jets*. VSP, The Netherlands, 1989, p.419.
31. KUDINOV, V. V., PEKSHEV, P. Yu & SAFINLLIN, V. A., In *High Temperature Dust Laden Jets*. VSP, The Netherlands, 1989, p.381.
32. LYAGUSHKIN, V. P., SOLOLENKO, O. P., PEKSHEV, P. Yu & SAFINLLIN, V. A., In *High Temperature Dust Laden Jets*. VSP, The Netherlands, 1989, p.285.

33. ROBERTS, K. A. & CLYNE, T. W., *Surface Coat. Technol.*, **41** (1990) 103.
34. BIANCHI, L., MELLALI, M., GRIMAUD, A., FAUCHAIS, P. & LUCCHESI, P., In *Proc. 11th Int. Symp. on Plasma Chemistry* (ed. J. Harry, University of Loughborough, UK), **1** (1993) 172.
35. BIANCHI, L., VARDELLE, M., VARDELLE, A., BLEIN, F., LUCCHESI, P. & FAUCHAIS, P., In *Thermal Spray Industrial Applications (Pat.)*. ASM Int., OH, USA, 1996, p.569.
36. MOREAU, C., CIELO, P., LAMONTAGNE, M., DALLAIRE, S. & VARDELLE, M., *Meas. Sci. Technol.*, **1** (1990) 807.
37. FANTASSI, S., VARDELLE, M., FAUCHAIS, P. & MOREAU, C., In *Thermal Spray: International Advances in Coatings Technology*. ASM Int., OH, USA, 1992, p.755.
38. FANTASSI, S., VARDELLE, M., VARDELLE, A. & FAUCHAIS, P., *J. Thermal Spray Technol.*, **2**(4) (1993) 379.
39. SPJUT, R. E., *Optical Eng.*, **26** (1987) 467.
40. MOREAU, C., CIELO, P. & LAMONTAGNE, M., *J. Thermal Spray Technol.*, **1**(4) (1992) 317.
41. BIANCHI, L., GRIMAUD, A., BLEIN, F., LUCCHESI, P. & FAUCHAIS, P., In *Thermal Spray Industrial Applications (Pat.)*. ASM Int., OH, USA, 1996, p.575.
42. COUDERT, J. F., PLANCHE, M. P., BETOULE, O., VARDELLE, M. & FAUCHAIS, P., In *Plasma Spraying Theory and Applications*. ASM Int., OH, USA, 1993, p.19.
43. MOREAU, C., GOUGEON, P. & LAMONTAGNE, M., *J. Thermal Spray Technol.*, **4**(1) (1995) 25.